

⁷⁵As NMR study of antiferromagnetic fluctuations in Ba(Fe_{1-x}Ru_x)₂As₂

Tusharkanti Dey, P. Khuntia, A.V. Mahajan*

Department of Physics, IIT Bombay, Powai, Mumbai 400076, India

Shilpam Sharma, A. Bharathi

Condensed Matter Physics Division, Materials Science Group,

Indira Gandhi Centre for Atomic Research (IGCAR), Kalpakkam 603102, India

Abstract

Evolution of ⁷⁵As NMR parameters with composition and temperature was probed in the Ba(Fe_{1-x}Ru_x)₂As₂ system where Fe is replaced by isovalent Ru. While the Ru-end member was found to be a conventional Fermi liquid, the composition ($x = 0.5$) corresponding to the highest T_c (20 K) in this system shows an upturn in ⁷⁵As $\frac{1}{T_1T}$ below about 80 K evidencing the presence of antiferromagnetic (AFM) fluctuations. These results are similar to those obtained in another system with isovalent substitution BaFe₂(As_{1-x}P_x)₂ [Y. Nakai, T. Iye, S. Kitagawa, K. Ishida, H. Ikeda, S. Kasahara, H. Shishido, T. Shibauchi, Y. Matsuda, and T. Terashima, Phys. Rev. Lett. **105**, 107003 (2010)] and point to the possible role of AFM fluctuations in driving superconductivity.

PACS numbers: 74.70.Xa, 74.25.nj, 74.62.Dh, 74.62.-c

1. Introduction

The recent discovery of superconductivity in an iron based material [1] LaFeAs(O_{1-x}F_x) with a superconducting transition temperature $T_c = 26$ K and soon after, the increase of T_c to 43 K with applied pressure [2] has reignited the interest in superconductors. The main motivating factors for this interest are (i) the presence of Fe, which is normally not considered conducive to superconductivity and (ii) the superficial similarity to the high- T_c cuprates, in terms of the existence of FeAs layers.

The parent compound BaFe₂As₂ is a semimetal which crystallizes in a ThCr₂Si₂-type structure ($I4/mmm$) and exhibits a spin-density-wave (SDW) transition [3] at ~ 140 K. Superconductivity is induced following electron/hole doping [4, 5], by applying pressure externally [6], by replacing As with isovalent P [7], or by replacing Fe with isovalent Ru [8].

Heterovalent substitutions manifestly give rise to a change in the carrier concentration in addition to other effects. Therefore, it appears interesting to investigate isovalent substitutions which might help to narrow down the relevance of various factors to superconductivity. Perhaps with this motivation, Ru substitution at the Fe site was attempted [8–10]. In the reported works relevant to single crystals, the authors were able to substitute Ru in place of Fe, however, only up to a limit of $x = 0.37$ (in [9]) and $x = 0.5$ (in [10]). Very recently, Eom *et al.* [11] prepared single crystals upto $x = 0.7$. On the other hand, in the work on polycrystalline Ba(Fe_{1-x}Ru_x)₂As₂ by S. Sharma *et al.* [8] complete substitution was achieved. In Sr(Fe_{1-x}Ru_x)₂As₂ as well Schnelle *et al.* [12] achieved full substitution of Fe with Ru in polycrystalline samples. Ru substitution suppresses the long-range antiferromagnetic transition and superconductivity appears. The role

played by antiferromagnetic spin fluctuations has been suggested to be important towards a pairing mechanism.

From magnetic susceptibility measurements, Nath and co-workers [13] have estimated the density-of-states at the Fermi level $D(\epsilon_F)$ of BaRu₂As₂ to be 2.1 states/(eV formula unit). Thaler *et al.* have done a detailed study on single crystalline Ba(Fe_{1-x}Ru_x)₂As₂ samples where they have shown the similarity of its phase diagram with that of BaFe₂As₂ with pressure [9]. Brouet *et al.* [14] have studied a Ba(Fe_{0.65}Ru_{0.35})₂As₂ single crystal using electrical transport and photoemission spectroscopy and concluded that the electron and hole concentrations were equal to each other but double of those in BaFe₂As₂. The increase in carrier concentration has been attributed to a large change in the band structure as compared to undoped BaFe₂As₂. From thermal conductivity measurements on Ba(Fe_{0.64}Ru_{0.36})₂As₂ single crystal and comparing their data with other doping samples, Qiu *et al.* [15] have shown that nodal superconductivity induced by isovalent doping (P at As site and Ru at Fe site) have the same origin. From electrical transport measurements, Eom *et al.* [11] suggest that whereas there is a deviation from Fermi-liquid behavior for compositions around the maximum T_C , overdoped compositions tend towards a Fermi-liquid behavior. However, due to the difficulty in preparing single crystals of BaRu₂As₂ no comparison exists between the superconducting compositions and the Ru end member.

Nuclear magnetic resonance (NMR) has been instrumental in the case of cuprates in detecting antiferromagnetic fluctuations, pseudo-gap, and other features. In the FeAs compounds as well, NMR has been extensively used to obtain a deeper understanding of various physics issues [16]. In fact, in the isovalent substituted system BaFe₂(As_{1-x}P_x)₂, ³¹P NMR was found to show the prominence of antiferromagnetic fluctuations above T_c in the superconducting compositions [17]. However, up to now, no local probe investigations have been reported

*Electronic address: mahajan@phy.iitb.ac.in

which might help to understand the variation of properties in the $\text{Ba}(\text{Fe}_{1-x}\text{Ru}_x)_2\text{As}_2$ system. In this paper, we report ^{75}As NMR measurements on $\text{Ba}(\text{Fe}_{1-x}\text{Ru}_x)_2\text{As}_2$ ($x = 0, 0.25, 0.5, 1$) samples. From our measurements, we show that the Ru-end member behaves like a conventional Fermi liquid. In contrast, for the $x = 0.5$ sample ($T_c^{(\text{onset})} = 20\text{ K}$), ^{75}As $\frac{1}{T_1T}$ is constant at high- T but increases with decrease in T below 80 K suggesting the emergence of antiferromagnetic fluctuations. Also, no evidence of heavy Fermi liquid behaviour in $\text{Ba}(\text{Fe}_{1-x}\text{Ru}_x)_2\text{As}_2$ is found from our NMR measurements.

2. Experimental Details

Polycrystalline samples of $\text{Ba}(\text{Fe}_{1-x}\text{Ru}_x)_2\text{As}_2$ ($x = 0, 0.25, 0.5, 1$) were prepared at IGCAR as detailed in [8]. Basic characterisation of the samples was done by x-ray diffraction, magnetization, and resistivity measurements. For NMR measurements, we tried to align the powder samples by mixing with Stycast 1266 epoxy and then curing overnight in an external magnetic field $H = 93.954\text{ kOe}$. ^{75}As NMR measurements were carried out at IIT Bombay using a Tecmag pulse spectrometer in a magnetic field of 93.954 kOe using a room-temperature bore Varian superconducting magnet. Variable temperature measurements were performed using an Oxford continuous flow cryostat, using liquid nitrogen in the temperature range 80 – 300 K and using liquid helium in the temperature range 4 – 80 K. The ^{75}As has nuclear spin $I = \frac{3}{2}$ (100% natural abundance) and gyromagnetic ratio $\frac{\gamma}{2\pi} = 7.2919\text{ MHz/T}$. Spectra were obtained by Fourier transform of the spin echo resulting from a $\frac{\pi}{2} - \tau - \frac{\pi}{2}$ pulse sequence. Spin-lattice relaxation time (T_1) was obtained by fitting the time dependence of spin-echo intensity $m(t)$ with the formula

$$1 - m(t)/m(\infty) = A \exp(-t/T_1) + B \exp(-6t/T_1) \quad (1)$$

following a $\frac{\pi}{2} - t - (\frac{\pi}{2} - \frac{\pi}{2})$ sequence where the $\frac{\pi}{2}$ pulse duration is $\sim 4\mu\text{s}$.

3. Results and discussions

X-ray powder diffraction revealed the presence of small amount (several percent) of FeAs as also unreacted Fe and Ru present in the samples. The average Ru content is expected to be less than the nominal amount as was already found by others [9, 10]. Another point to note is that the x-ray diffraction peaks for our $x = 0.5$ sample are broad compared to those of the end-members. This is likely due to a distribution of Ru content for this sample. Similar broadened peaks were also found in $\text{Sr}(\text{Fe}_{1-x}\text{Ru}_x)_2\text{As}_2$ [18]. The inability of Thaler *et al.* [9] and Rullier-Albenque *et al.* [10] to obtain homogeneous single crystals of $\text{Ba}(\text{Fe}_{1-x}\text{Ru}_x)_2\text{As}_2$ with $x > 0.21$ is perhaps related to the difficulty in obtaining a sharply defined composition. In any case, whereas a small amount of extrinsic impurity or a distribution of Ru content does affect bulk properties like magnetisation and resistivity, using a local probe such as NMR we will be able to probe the intrinsic properties.

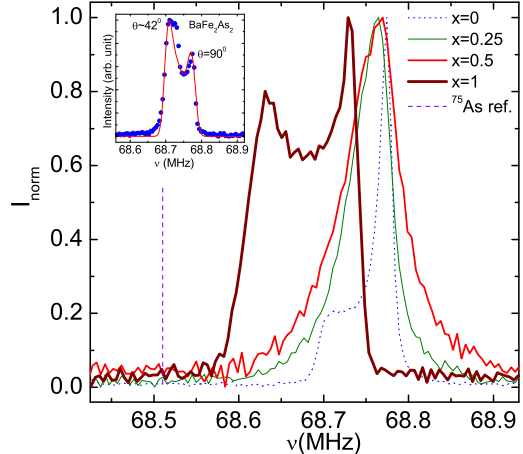


Figure 1: ^{75}As NMR spectra measured at room temperature in a fixed field 93.954 kOe for all four $\text{Ba}(\text{Fe}_{1-x}\text{Ru}_x)_2\text{As}_2$ samples. The ^{75}As reference frequency is marked by a dashed vertical line. Inset: ^{75}As NMR spectrum for a randomly oriented powder sample of BaFe_2As_2 (blue dots). The simulated spectrum (red line) for the central line for $\nu_Q = 3.028\text{ MHz}$ and $\eta = 0$ (see text).

Resistivity and magnetic susceptibility (not shown here) evidence the occurrence of superconductivity in the BaFeRuAs_2 ($x = 0.5$) sample with a transition onset at $\sim 20\text{ K}$ similar to [8]. Following this basic characterisation, we investigate the normal state properties using ^{75}As NMR as a local probe. Before describing our measurements, we will first state some basic facts pertaining to the NMR of ^{75}As nuclei. In the $\text{Ba}(\text{Fe}_{1-x}\text{Ru}_x)_2\text{As}_2$ system, ^{75}As ($I = \frac{3}{2}$) is not at a site of cubic symmetry. This gives rise to a non-zero electric field gradient (EFG) at the ^{75}As site and coupled with its electric quadrupole moment, there arise changes in the NMR lineshape as also the spin-lattice relaxation behaviour. When the quadrupole term in the Hamiltonian is weak compared to the Zeeman term it is enough to consider the effects upto first order in perturbation theory. In this case, the central line ($\frac{1}{2} \leftrightarrow -\frac{1}{2}$ transition) is unaffected while satellite lines appear corresponding to the $-\frac{3}{2} \leftrightarrow -\frac{1}{2}$ and $\frac{3}{2} \leftrightarrow \frac{1}{2}$ transitions. The positions of the satellite lines depends on the angle θ between the magnetic field direction and the direction made by the maximum of the EFG V_{zz} . When quadrupole effects are considered to second order

(and for axial symmetry), the central line position (in the absence of anisotropy) also depends on θ and is given by the following equation

$$\nu_{(\pm\frac{1}{2})}^{(2)} = \nu_0 + \frac{\nu_Q^2}{32\nu_0} \left[I(I+1) - \frac{3}{4} \right] (1 - \cos^2\theta)(9\cos^2\theta - 1) \quad (2)$$

where ν_Q is the quadrupole frequency and ν_0 the Larmor frequency. In a randomly aligned polycrystalline sample the central lineshape is the powder average, resulting in two peaks corresponding to $\theta \approx 41.8^\circ$ and $\theta = 90^\circ$. It is known [19] that ν_Q for BaFe_2As_2 is about 3 MHz. The central line pattern in our randomly aligned BaFe_2As_2 sample can be generated (see inset of figure 1) taking $\nu_Q = 3.028$ MHz. In going from BaFe_2As_2 to BaRu_2As_2 these numbers are expected to change only nominally.

We have attempted to align the samples with the *ab*-plane in the applied field direction. As seen from the contrast between the figure 1 inset (randomly aligned) and the curve for $x = 0$ (aligned sample) in the main figure 1, this is well achieved for BaFe_2As_2 . However, it appears that the Ru-substituted samples did not align in the field. This arises perhaps due to the absence of single crystallites in the powders. Nevertheless, our objectives from the spectra measurements are twofold; (i) to determine the Knight shift as a function of temperature and (ii) to irradiate the central line and then determine the spin-lattice relaxation rate. From the position of the $\theta = 90^\circ$ peak, the shift can be determined. Since the central line is only about 200 kHz in overall extent whereas our typical $\frac{\pi}{2}$ pulsewidth is $4\mu\text{s}$, there is sufficient spectral width to saturate the central line with a single $\frac{\pi}{2}$ pulse.

The measured spectra could be simulated assuming $K_x = K_y \approx K_z = K$, $\nu_Q = 3.028$ MHz and $\eta = 0$ (i.e., $V_{xx} = V_{yy}$). The isotropic shift is therefore determined using equation 2 ($K = \frac{\nu_0 - \nu_{ref}}{\nu_{ref}}$). K gives useful information about the intrinsic susceptibility (having both spin and orbital contributions) of the sample. We have $K = K_{spin} + K_{chem}$, where $K_{spin} = \frac{A_{hf}\chi_{spin}}{N_A\mu_B}$ is the spin part of the Knight shift and K_{chem} is the temperature independent chemical shift. The hyperfine coupling is A_{hf} while N_A and μ_B are the Avogadro number and the Bohr magneton, respectively. The temperature variation of shift is shown in figure 2. As to the value of the chemical shift, there is some disagreement in literature. Ning *et al.* [20] estimated the chemical shift from their measurement at 4.2 K. On the other hand, Kitagawa *et al.* [21] obtained chemical shift by plotting $K - \chi$ and then extrapolating to zero susceptibility. Kitagawa *et al.* commented that the value of $K_{chem} \sim 0.2\%$ (also found by Ning *et al.*) seemed rather large and perhaps the extrapolation was not reliable. In view of this as also the possibility that K_{chem} might be composition dependent, we have not corrected our shift data for the chemical shift.

For $x = 1$, the shift is almost independent of tem-

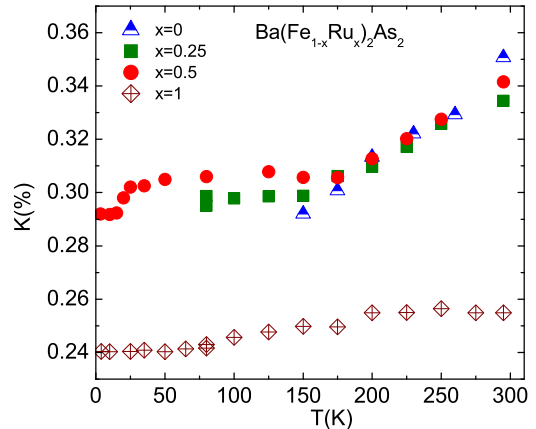


Figure 2: Shift for various compositions is shown as a function of temperature T . For the metallic one ($x = 1$) the shift K is nearly independent of T . For $x = 0.5$ the superconducting transition is manifested by a step like change in the K .

perature like a conventional Fermi liquid. For the other three samples (including the superconducting composition) the shift value is higher than that for $x = 1$. Further it increases linearly with temperature above 160 K. Below 160 K the shift is independent of temperature for $x = 0.25$ and $x = 0.5$ samples. The drop in shift at ~ 20 K for $x = 0.5$ is due to the superconducting transition. The SDW transition is seen at 140 K and 70 K for $x = 0$ and 0.25, respectively. The nearly unchanged shift in going from $x = 0$ to $x = 0.5$ indicates that the density-of-states at the Fermi level $D(\epsilon_F)$ remains unchanged with substitution up to $x = 0.5$. On the other hand, the non-superconducting, metallic end-member has a significantly smaller shift (and therefore $D(\epsilon_F)$). In case K_{chem} is taken to be about 0.2% (as in [20]) the reduction in K_{spin} is by a factor of two in going from $x = 0.5$ to $x = 1$. A similar trend is seen in $\text{BaFe}_2(\text{As}_{1-x}\text{P}_x)_2$ for the larger values of x beyond the superconducting dome [17].

To study the low-energy spin dynamics, T_1 is measured as a function of temperature for all the samples by the saturation recovery method. A representative data-set for BaRu_2As_2 at 50 K and its fit with equation 1 is shown in the inset of figure 3.

For the $x = 1$ sample, the data could be fit with $A : B = 1 : 9$ in the full temperature range as also for

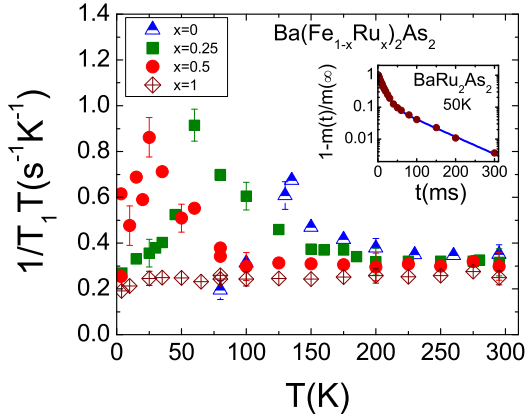


Figure 3: ^{75}As spin-lattice relaxation rate divided by temperature ($\frac{1}{T_1 T}$) is shown as a function of temperature (typical error bars are shown). Inset: The recovery of the ^{75}As nuclear magnetization (wine color dots) for BaRu_2As_2 at 50 K and its fit (blue line) with Eq. 1 with $A = 0.1$ and $B = 0.9$.

other compositions for temperatures higher than about 60 K. At lower temperatures the ratio of the coefficients is about 4 : 6. The ratio of the coefficients is expected to be different from 1 : 9 in case the relaxation is not magnetic. In the present case, it is possible that the lattice becomes soft prior to the superconducting transition and then quadrupolar relaxation also contributes. However, there could be other possibilities. The variation of the relaxation rate divided by temperature as a function of temperature is shown in figure 3. Note that conventional, wide-band metallic systems will have a T -independent K_{spin} . Therefore, Korringa behaviour (T -independent $K_{spin}^2 T_1 T$) in a conventional metal implies the constancy of $\frac{1}{T_1 T}$ with T . For the non-superconducting $x = 1$ composition, $\frac{1}{T_1 T}$ is seen to be independent of T down to 4 K. It's shift is also found to be only weakly T -dependent. Of course, one needs to know K_{chem} in order to make a quantitative comment about the T -variation of K_{spin} and consequently of $K_{spin}^2 T_1 T$. Since the present problem involves transferred hyperfine inter-

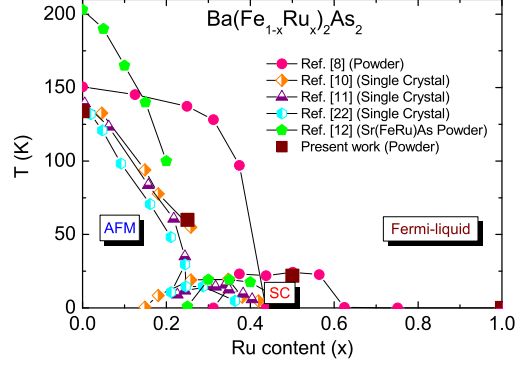


Figure 4: Phase diagrams for powder (solid symbol) and single crystal (half-filled symbol) samples of $\text{Ba}(\text{Fe}_{1-x}\text{Ru}_x)_2\text{As}_2$ available in literature, are shown. Phase diagram $\text{Sr}(\text{Fe}_{1-x}\text{Ru}_x)_2\text{As}_2$ powder sample is also shown. Different regions of the phase diagram are marked based on the NMR parameters obtained from our measurements.

actions, the relaxation rate may also be affected by the form factor (q -dependence of hyperfine couplings) which could lead to a deviation from the free-electron value of $K_{spin}^2 T_1 T$ as also its expected T -independence. Our observed value of $K_{spin}^2 T_1 T$ for $x = 1$ is within an order of magnitude of the free electron value and is also nearly T -independent which, keeping the above limitations in mind, seems to suggest the validity of the Fermi-liquid picture for BaRu_2As_2 . It's worth mentioning that Eom *et al.* [11] also found Fermi-liquid behavior for higher doping ($x \sim 0.7$) samples. In contrast, for the superconducting sample ($x = 0.5$) ($\frac{1}{T_1 T}$) is independent of T down to about 80 K below which it shows an upturn before dropping at the superconducting transition at $T \sim 20$ K. The upturn in ($\frac{1}{T_1 T}$) as a function of temperature has also been seen (in the context of iron pnictides) in $\text{BaFe}_2(\text{As}_{1-x}\text{P}_x)_2$ in ^{31}P NMR studies [17] and is believed to signify the existence of antiferromagnetic fluctuations. For $x = 0$ and 0.25, ($\frac{1}{T_1 T}$) shows an anomaly at the SDW transition which is also seen in shift measurements. Compiling the published data on $\text{Ba}(\text{Fe}_{1-x}\text{Ru}_x)_2\text{As}_2$ (single crystals and powders), we summarize its magnetic phase diagram in figure 4. Data for $\text{Sr}(\text{Fe}_{1-x}\text{Ru}_x)_2\text{As}_2$ are also shown for reference. The heavily overdoped region exhibits Fermi-liquid behavior and near the top of the superconducting dome, there is a prominence of AFM fluctuations along with non-Fermi-liquid behavior based on the NMR data. The AFM/SDW part shows anomalies in the shift at the ordering temperature as expected.

4. Conclusions

We have reported ^{75}As NMR measurements on $\text{Ba}(\text{Fe}_{1-x}\text{Ru}_x)_2\text{As}_2$ ($x = 0, 0.25, 0.5, 1$) samples for the first time. The full ruthenated sample ($x = 1$) is a conventional Fermi liquid as evidenced from shift and T_1

measurements. On moving towards the superconducting composition ($x = 0.5$), the density-of-states at the Fermi level increases. Further, for the $x = 0.5$ sample, $\frac{1}{T_1 T}$ shows an upturn with decreasing temperature indicative of the emergence of antiferromagnetic fluctuations. Our results suggest the importance of AFM fluctuations in

the superconducting mechanism in the FeAs-based systems. Similar results have been reported for isovalent P-substitution at the As site [17].

5. Acknowledgments

We thank the Department of Science and Technology, India for financial support.

-
- [1] Kamihara Y, Watanabe T, Hirano M and Hosono H 2008 *J. Am. Chem. Soc.* **130** 3296
 - [2] Takahashi H, Igawa K, Arii K, Kamihara Y, Hirano M and Hosono H 2008 *Nature (London)* **453** 376
 - [3] Rotter M, Tegel M, Johrendt D, Schellenberg I, Hermes W and Pottgen R 2008 *Phys. Rev. B* **78** 020503(R)
 - [4] Sefat A S, Jin R, McGuire M A, Sales B C, Singh D J and Mandrus D 2008 *Phys. Rev. Lett.* **101** 117004
 - [5] Rotter M, Tegel M and Johrendt D 2008 *Phys. Rev. Lett.* **101** 107006
 - [6] Alireza P L, Ko Y T C, Gillett J, Petrone C M, Cole J M, Lonzarich G G and Sebastian S E 2009 *J. Phys.: Condens. Matter* **21** 012208
 - [7] Jiang S, Xing H, Xuan G, Wang C, Ren Z, Feng C, Dai J, Xu Z and Cao G 2009 *J. Phys.: Condens. Matter* **21** 382203
 - [8] Sharma S, Bharathi A, Chandra S, Reddy V R, Paulraj S, Satya A T, Sastry V S, Gupta A and Sundar C S 2010 *Phys. Rev. B* **81** 174512
 - [9] Thaler A, Ni N, Kracher A, Yan J Q, Budko S L and Canfield P C 2010 *Phys. Rev. B* **82** 014534
 - [10] Rullier-Albenque F, Colson D, Forget A, Thuery P and Poissonnet S 2010 *Phys. Rev. B* **81** 224503
 - [11] Eom M J, Na S W, Hoch C, Kremer R K, and Kim J S 2011 arXiv:1109.1083v1
 - [12] Schnelle W, Leithe-Jasper A, Gumeniuk R, Burkhardt U, Kasinathan D and Rosner H 2009 *Phys. Rev. B* **79** 214516
 - [13] Nath R, Singh Y and Johnston D C 2009 *Phys. Rev. B* **79** 174513
 - [14] Brouet V, Rullier-Albenque F, Marsi M, Mansart B, Aichhorn M, Biermann S, Faure J, Perfetti L, Taleb-Ibrahimi A, Fevre P L, Bertran F, Forget A and Colson D 2010 *Phys. Rev. Lett.* **105** 087001
 - [15] Qiu X, Zhou S Y, Zhang H, Pan B Y, Hong X C, Dai Y F, Eom M J, Kim J S, Li S Y 2011 arXiv:1106.5417v2
 - [16] Ishida K, Nakai Y and Hosono H 2009 *J. Phys. Soc. Jpn.* **78** 062001
 - [17] Nakai Y, Iye T, Kitagawa S, Ishida K, Ikeda H, Kasahara S, Shishido H, Shibauchi T, Matsuda Y and Terashima T 2010 *Phys. Rev. Lett.* **105** 107003
 - [18] Qi Y, Wang L, Gao Z, Wang D, Zhang X and Ma Y 2009 *Physica C* **469** 1921
 - [19] Baek S -H, Klimczuk T, Ronning F, Bauer E D, Thompson J D and Curro N J 2008 *Phys. Rev. B* **78** 212509
 - [20] Ning F, Ahilan K, Imai T, Sefat A S, Jin R, McGuire M A, Sales B C and Mandrus D 2009 *J. Phys. Soc. Jpn.* **78** 013711
 - [21] Kitagawa K, Katayama N, Ohgushi K, Yoshida M and Takigawa M 2008 *J. Phys. Soc. Jpn.* **77** 114709
 - [22] Kim M G, Pratt D K, Rustan G E, Tian W, Zarestky J L, Thaler A, Bud'ko S L, Canfield P C, McQueeney R J, Kreyssig A and Goldman A I 2011 *Phys. Rev. B* **83** 054514